Photoinduced diradical formation and decay in uncomplexed and metal-bound benzotriazine systems: mechanistic implications to chemically and biologically relevant photochemistry

Brian J. Kraft and Jeffrey M. Zaleski*

Department of Chemistry, Indiana University, Bloomington, Indiana 47405, USA.
E-mail: zaleski@indiana.edu

Received (in New Haven, CT, USA) 21st May 2001, Accepted 1st July 2001
First published as an Advance Article on the web 11th September 2001

The photochemical reactivities of 3-hydroxy-1,2,3-benzotriazine-4(3*H*)-one (**1a**) and tris[3-hydroxy-1,2,3-benzotriazine-4(3*H*)-one]iron(III) (**1b**) have been studied in solution and low temperature (5–77 K) glasses. Photoexcitation ($\lambda \geqslant 345$ nm) of **1a** and **1b** ultimately results in population of a ligand-centered excited state that releases N_2. Electron paramagnetic resonance reveals the presence of $S = 1$ and $S = 0$ diradical intermediates upon photolysis of **1a** and **1b**, respectively, at 4 K. These species convert to an $S = 1/2$, nitrogen-centered monoradical species ($a_N = 23$ G) upon warming to 77 K *via* H-atom abstraction from the matrix. In solution, the first intermediates observed upon photolyses ($\lambda = 355$ nm) of **1a** and **1b** are oxime ketenes (**5**: $\lambda = 385$, 440 nm; **9**: $\lambda = 390$, 430, 740 nm) that are formed from collapse of the diradical to generate a 4-membered β-lactam ring. The decay kinetics for the oxime ketene **5** decay can be fitted to a biexponential expression representing a parallel reaction mechanism with an element of reversibility. Thus, the data proposes the existence of an equilibrium between the oxime ketene and the spectroscopically silent β-lactam intermediate, as well as a first or pseudo first-order solvent-dependent pathway for the oxime ketene. The kinetics for formation and decay of the ketene are strongly influenced by the presence of the Fe(III) center, which leads to an increase in the lifetime of the diradical in solution, and a retarded rate of formation for the oxime ketene **9**. The solution lifetimes suggest that the diradical intermediates only persist sufficiently long to react with bound solution substrates, whereas the ketene intermediates have suitable kinetic viabilities to react bimolecularly in solution.

Introduction

The thermal or photochemical generation of radical intermediates and their subsequent reactivities are fundamentally important for understanding chemical transformations in the fields of organic, inorganic, and biological chemistries. In addition to basic research interests in these areas, the investigation of diradical reactivity has also evolved due to the potential for practical uses of these highly energetic starting materials. Diazenes,[1] terminal diazo compounds,[2] and benzotriazole[3] derivatives have been employed as reagents for synthetic chemistry and also as resists in photolithography applications.[4,5] Moreover, the discovery of the kinamycin family of natural products,[6,7] and their roles in DNA cleavage chemistry has further extended interest in the thermal and photochemical reactivities of synthetic analogs such as 9-diazofluorene,[8] benzotriazole,[9,10] and various diazo ketones.[11]

Metal ions, by virtue of their ability to adopt variable redox states and stabilize unpaired electrons can also participate in and, more importantly, induce ligand-based radical reactivity. This frequently occurs *via* intramolecular thermal or photochemical charge transfer reactions. Important examples include the preparation of metal–semiquinone ligand radical complexes, which serve as novel magnetic molecules,[12] and metal–phenol radical structures that mimic key intermediates in the galactose oxidase family of enzymes.[13,14] The metal–ligand charge transfer excited state luminescence[15] and subsequent DNA degrading reactivity[16] of $[Ru(bpy)_3]^{2+}$ and related derivatives are also examples of the important role that metal–ligand radical reactivity can play in chemical and biological reactions.

The instability of diazo compounds to redox processes and the ability of metal ions to adopt variable redox states link seemingly disparate chemical reactivities; N_2 loss from organic diazo compounds and metal-based photochemistry. Cu(II) salts have been used in the thermal activation of terminal diazo units, which release N_2 and form Cu(I) as a synthetic strategy to couple organic fragments *via* radical pathways.[2] The radical intermediates generated by this reaction as well as those derived from the charge transfer induced photochemical activation of 3-hydroxy-1,2,3-benzotriazine-4(3*H*)-one by Fe(III),[17] have recently been used to modify DNA.[18,19] These examples document the central role that metal ions can play in the development of radical-based therapeutics.

Yet, fundamental questions exist regarding the precise mechanism of metal-mediated N_2 loss, relative to that from organic diazo analogs. Also of primary interest are the characteristics of the intermediates following N_2 loss, as well as the kinetic viabilities of these intermediates for performing unimolecular or bimolecular reactions with solution substrates. Many of these important mechanistic issues have not been thoroughly addressed. To this end, we report the photochemical reactivities of 3-hydroxy-1,2,3-benzotriazine-4(3*H*)-one (**1a**) and tris[3-hydroxy-1,2,3-benzotriazine-4(3*H*)-one]-iron(III) (**1b**) both in solution at ambient temperature, and in a 2-MeTHF glass from 4–77 K. The results document the formation of diradical intermediates at low temperatures and reveal important differences in the kinetics of evolution of the intermediates in solution. Finally, the reactivity of **1b** has

This journal is © The Royal Society of Chemistry and the Centre National de la Recherche Scientifique 2001

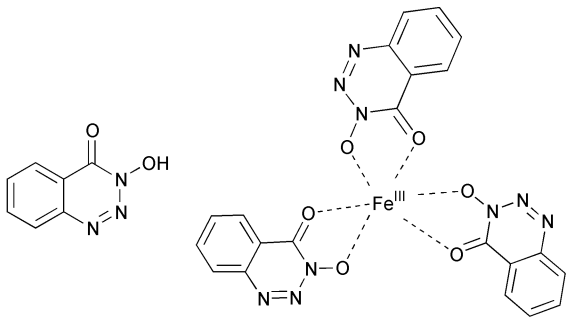

1a 1b

broader implications in the emerging research fields of photomedicine and environmentally relevant siderophore photochemistry.[20]

Experimental

Materials

Acetonitrile, benzonitrile and 2-methyltetrahydrofuran were of HPLC grade, while methanol and isopropyl alcohol were of spectroscopic grade. All solvents used in measurements were stored over activated 3 Å molecular sieves for at least 24 h prior to use. NMR solvents (acetonitrile-d_3, methanol-d_3) were also dried over 3 Å sieves prior to use. The ligand 3-hydroxy-1,2,3-benzotriazine-4-(3*H*)-one (**1a**) was purchased from Aldrich and the purity was confirmed by ^{1}H NMR, while tris(3-hydroxy-1,2,3-benzotriazine)iron(III) (**1b**) was prepared and characterized as previously described.[17]

Physical measurements

Samples were prepared using volumetric glassware, and standard Schlenk and drybox techniques. Solvents were degassed by either purging with N_2 for >1 h, or several freeze–pump–thaw cycles. Electron paramagnetic resonance (EPR) spectra of the metal compound and free ligand were obtained with solution concentrations of *ca.* 2 mM, while the transient absorption experiments were performed at concentrations of *ca.* 6 mM for **1a**, and 1–2 mM for the corresponding iron complex **1b**.

Electronic absorption spectra were collected on a Perkin-Elmer Lambda 19 UV/VIS/NIR spectrometer at ambient temperature. Fluorescence measurements were made using a Perkin Elmer LS 50 B luminescence spectrometer equipped with a Hamatatsu model R2371 PMT. Infrared spectra were recorded on a Nicolet 510P FT-IR spectrometer. ^{1}H and $^{13}C\{^1H\}$ NMR spectra were measured on a Varian VXR 400 spectrometer and referenced to the residual solvent signal. All EPR spectra were recorded at X-band (9.5 GHz) on an ESP 300 Bruker spectrometer. Typical EPR conditions: microwave power, 10 mW; modulation amplitude, 5–20 G; modulation frequency, 100 kHz; receiver gain; (2–5) × 10^4. EPR spectra were simulated using a Monte Carlo method.[21,22] Matrix photolyses were performed directly in the EPR cavity with a 150 W Hg source coupled *via* a liquid light pipe (Oriel #77557). Photolyses were performed at $\lambda \geqslant 345$ nm, where the cutoff wavelength was selected using a series of long wavelength pass filters (295, 320 and 345 nm). EPR spectra were obtained after photolysis times ranging from 5 min to 1 h and are plotted after the spectral subtraction of a control sample containing a small amount of photogenerated matrix radical. Quantum yield measurements for the photochemical reaction of **1b** are reported relative to $K_3[Fe(C_2O_4)_3]$ and were monitored by the bleaching of the electronic spectrum at 435 nm.[17]

Transient absorption measurements were performed using the third harmonic of a Coherent Infinity 40-100 pulsed Nd : YAG laser operating at a repetition rate of 12 Hz (FWHM = 5 ns) and an energy of *ca.* 2 mJ pulse^{-1}. The probe beam originated from a PTI model LPS-220 water cooled 150 W Xe arc lamp and was chopped at a rate of 12 Hz (FWHM *ca.* 40 ms). White light was used to trigger the photolysis pulse, which was synchronized in time using a delay generator. The pump and probe beams converged on a 2 mm quartz cell at *ca.* 20°. The probe beam was then focused onto the entrance slit of an ISA model 340S single monochromator (grating: 1200 groove mm^{-1}), equipped with a Hamamatsu R928P photomultiplier tube. The output from the photomultiplier was fed through a variable gain broadband amplifier and recorded on a Tektronix (TDS 380) digital oscilloscope. Fluorescence from **1a** and benzonitrile resulted in the detection of a sharp (FWHM < 10 ns) bleach in the temporal profiles of **1a** and **1b**. Control experiments demonstrated that this had no effect on the rising edge of the observed transients and, for clarity, these features have been filtered from the temporal profiles.

Photolyses of 1a and 1b

Photolysis of 1a in $CH_3CH(OH)CH_3$. A solution of **1a** (400 ml, 20 mM) was photolysed with a 1000 W Xe lamp using 295, 320 and 345 nm cutoff filters in a Pyrex Schlenk flask for 12 h at 288 K. After removal of the solvent *in vacuo*, the crude photoproduct was dissolved in *ca.* 100 ml CH_2Cl_2. Unreacted starting material was then recovered by crystallization, with filtration affording 5.82 × 10^{-3} mol of **1a**. The filtrate volume was then reduced and the remaining material was separated on silica gel, using a 1 : 1 hexanes–ethyl acetate mobile phase. Of the total 378 mg of material recovered, 275 mg (1.41 × 10^{-3} mol, 65% of mol reacted) was identified as isopropyl *o*-hydroxyaminobenzoate ($C_{10}H_{13}NO_3$). ^{1}H NMR (CD_3OD): δ 9.24 (bs, 1H); 7.87 (d, 1H); 7.94 (t, 1H); 7.32 (d, 1H); 6.85 (d, 1H); 6.69 (bs, 1H); 5.16 (sept, 1H); 1.31 (d, 6H). ^{13}C NMR (CD_3OD): δ 169.8, 154.5, 135.1, 130.8, 119.5, 116.9, 114.5, 69.2, 22.0. MS (EI): *m/z* 195.2 [M^+, calc. for $C_{10}H_{13}NO_3$: 195.2]

Photolysis of 1b in C_6H_5CN. The iron complex, **1b** (1.10 × 10^{-3} mol) was dissolved in 500 ml of degassed benzonitrile. The resulting solution was then photolysed in 125 ml increments in a 150 ml Pyrex Schlenk flask at $\lambda \geqslant 345$ nm at 288 K for 9 h. After photolysis, all fractions were combined and the benzonitrile was removed *in vacuo*. The resulting red–orange solid was suspended in 200 ml methanol, and 3.35 × 10^{-3} mol of **1a** was added. The resultant slurry was allowed to stir overnight at room temperature. The brick red solid was then filtered off, dried and identified as **1b** (1.05 × 10^{-3} mol) by comparison of the IR spectrum to that of the starting material.[17] The solvent was then removed from the filtrate and the remaining material was dissolved in *ca.* 50 ml CH_2Cl_2. Excess **1a** was then removed by recrystallization (3.36 × 10^{-3} mol) and characterized by ^{1}H and ^{13}C NMR. The volume of the filtrate was reduced, and the mixture purified on silica gel using a 4 : 1 hexanes–ethyl acetate mobile phase. A pure white solid was isolated (14 mg) and identified as 2-aminobenzoic acid by comparison of the analytical data (^{1}H, ^{13}C NMR spectra and mass spectrum) to that of an authentic sample (Aldrich). The yield of this product based on mol of ligand reacted is 73%. ^{1}H NMR (CD_3OD): δ 7.82 (d, 1H); 7.20 (t, 1H); 6.71 (d, 1H); 6.56 (t, 1H); 5.30 (bs, 3H). ^{13}C NMR (CD_3OD): δ 171.6, 152.6, 135.0, 132.6, 117.7, 116.7, 111.6. MS (EI): *m/z* 137.1 [M^+, calc. for $C_7H_7NO_2$: 137.1].

Results

Electronic structures of 1a and 1b

The electronic absorption spectrum of **1a** has two strong, but poorly resolved features at 295 (ε = 5845) and 315 nm

($\varepsilon = 4484\ M^{-1}\ cm^{-1}$). Under basic conditions, these transitions undergo a bathochromatic shift (340, $\varepsilon = 6290$; 390 nm, $\varepsilon = 5061\ M^{-1}\ cm^{-1}$). Upon complexation of **1a** to a ferric center, the electronic absorption spectrum of **1b** develops a broad absorption feature centered at 430 nm ($\varepsilon = 6290\ M^{-1}\ cm^{-1}$) and a higher energy transition at 345 nm ($\varepsilon = 11\,573\ M^{-1}\ cm^{-1}$) (Fig. 1).

Photolysis of 1a

Low temperature EPR studies. Photolysis of **1a** in an ethanol matrix with $\lambda \geqslant 345$ nm at 4 K yields the EPR spectrum shown in Fig. 2(a): a clear 6-line pattern centered at $g = 2.0021$, a half-field transition is observed at $g = 4.0235$. The zero field splitting parameters $|D/hc| = 0.017\ cm^{-1}$ and $|E/hc| = 0.003\ cm^{-1}$ calculated directly from the spectrum suggest an inter-electron separation of *ca.* 5 Å.[23] Upon warming the sample to temperatures above 30 K, the half-field transition disappears and a new three line pattern centered at $g = 2.0037$ is observed [Fig. 2(b)]. Both the asymmetric splitting pattern and hyperfine coupling constant (a_N)[24] measured at 77 K ($a_N = 23$ G) are solvent independent.[25] Cooling the sample from 77 to 4 K yields a spectrum that is devoid of a half-field transition but exhibits a sharp signal centered at $g = 2.0035$ that is superimposed upon a very broad and ill-defined feature [Fig. 2(c)].

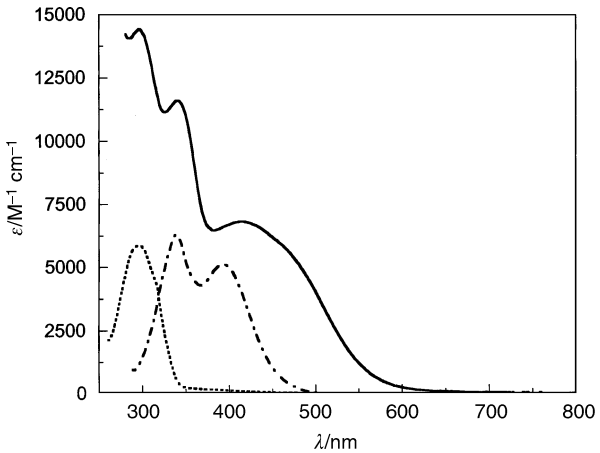

Fig. 1 Electronic absorption spectra of **1a** and **1b** in acetonitrile at 293 K; **1a** (···), deprotonated **1a** (–·–·–) and **1b** (——).

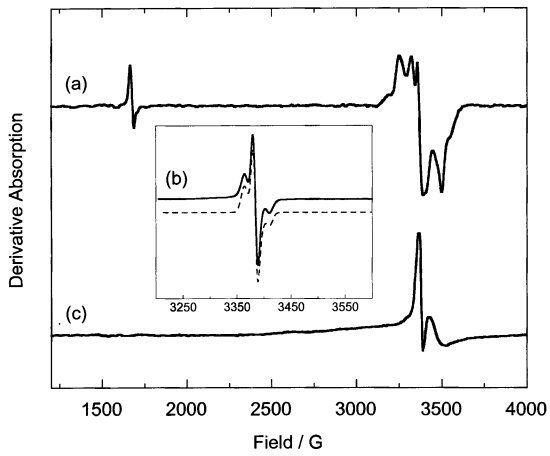

Fig. 2 EPR spectra of **1a** after 10 min of photolysis with $\lambda \geqslant 345$ nm in an ethanol glass at 4 K: (a) immediately following photolysis, (b) after warming to 77 K (——) along with simulation (– – –) (inset) and (c) after returning to 4 K.

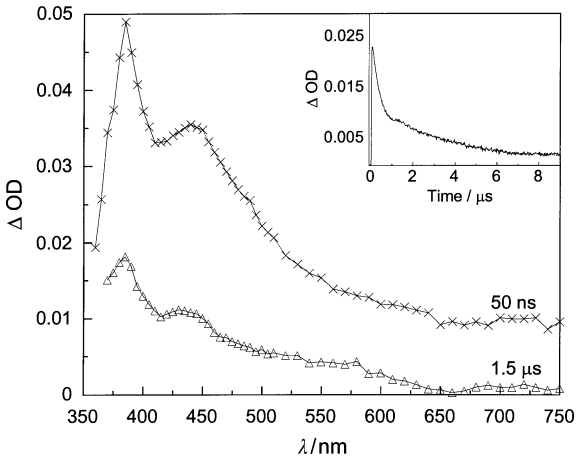

Fig. 3 Transient absorption spectrum of **1a** in acetonitrile taken at 50 ns (—×—) and 1.5 μs (—△—) after the 355 nm, 5 ns laser pulse. The temporal evolution of the absorption at 460 nm is shown in the inset.

Photoreactivity in solution. Upon excitation of **1a** in acetonitrile ($\lambda = 355$ nm), a single transient intermediate is immediately observed ($\lambda_{max} = 385$, 440 nm) that decays biexponentially ($\tau_1 \cong 277$ ns, $\tau_2 \cong 4.34$ μs) on the nanosecond-to-microsecond timescales (Fig. 3). In contrast, excitation of **1a** in 2-propanol yields two transients (Fig. 4), the first of which has a similar wavelength profile ($\lambda_{max} = 385$, 440 nm) to that observed for photolysis of **1a** in acetonitrile. In 2-propanol, this transient is rapidly quenched ($\tau_q \leqslant 30$ ns) to generate a second intermediate with a single absorption maximum at 380 nm that decays biexponentially ($\tau_{1'} \cong 588$ ns, $\lambda_{2'} \cong 6.67$ μs). When 10 molar equivalents of water are added as a proton source to dry acetonitrile, the rapid quenching is again observed (Fig. 5). Analysis of the products from a bulk photolysis performed in 2-propanol yields isopropyl *o*-hydroxyaminobenzoate (65%).

Photolysis of 1b

Low temperature EPR studies. Photolysis of **1b** at 4 K in a benzonitrile–2-MeTHF matrix results in the formation of an EPR silent species in the $g \approx 2$ region [Fig. 6(a)]. Warming the sample to 77 K with no additional photolysis results in a spectrum [Fig. 6(b)] that is nearly identical to that observed for the photolysis of **1a** at 77 K [Fig. 2(b)].

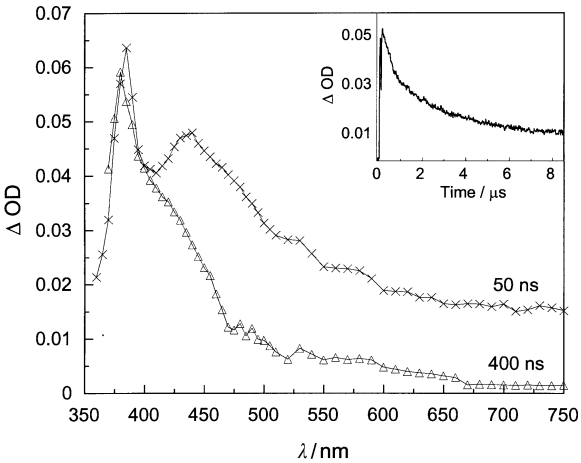

Fig. 4 Transient absorption spectrum of **1a** in 2-propanol taken at 50 (—×—) and 400 ns (—△—) after the laser pulse. The temporal evolution of the absorption at 390 nm is shown in the inset.

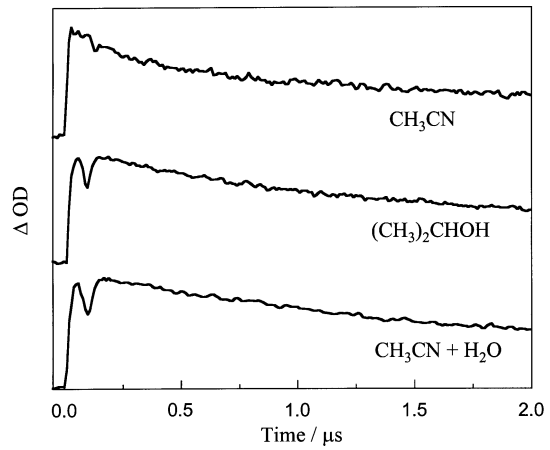

Fig. 5 A comparison of the short time features of the OD at 390 nm of **1a** in 2-propanol, acetonitrile and acetonitrile upon addition of 10 molar equivalents of water.

Photoreactivity in solution. Excitation of **1b** in benzonitrile ($\lambda = 355$ nm) yields a single transient that begins to form 240 ns ($k_f = 1.6 \times 10^6$ s^{-1}) after the pulse and has three absorption features at 390, 430 and 740 nm that decay monoexponentially ($k_d = 5.2 \times 10^5$ s^{-1}, Fig. 7). Analysis of the bulk photoproduct mixture, from photolysis in benzonitrile, after removal of the ferric center yields 2-aminobenzoic acid (73%).

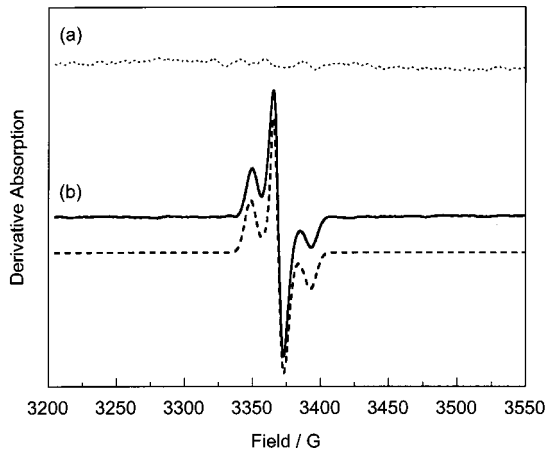

Fig. 6 EPR spectra of **1b** after 30 min of photolysis with $\lambda \geqslant 345$ nm in a 2-MeTHF–benzonitrile (1 : 1) glass at (a) 4 (···) and (b) 77 K (——), along with the simulated spectrum (– – –). The residual signal in the baseline of (a) derives from a small amount of matrix radical generated upon photolysis that is not completely removed by spectral subtraction.

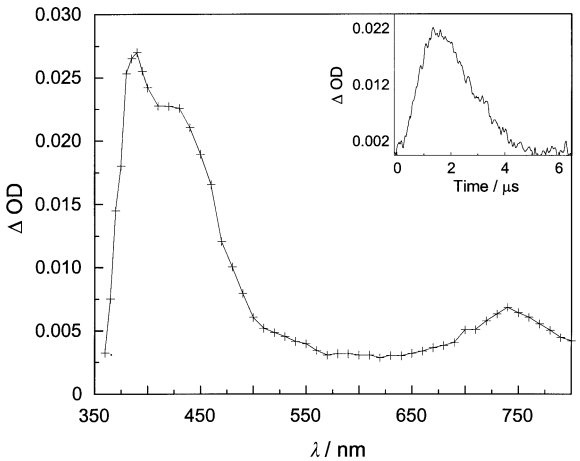

Fig. 7 Transient absorption spectrum of **1b** in benzonitrile taken at 1.5 μs (—+—) after the laser pulse. The temporal evolution of **9** at 430 nm is shown in the inset.

Discussion

Electronic structures of 1a and 1b

The electronic absorption spectrum of **1a** has two strong, but poorly resolved features at 295 ($\varepsilon = 5845$) and 315 nm ($\varepsilon = 4484$ M^{-1} cm^{-1}) that are derived from π–π* transitions within the conjugated framework (Fig. 1). Under basic conditions, these transitions undergo a bathochromatic shift (340, $\varepsilon = 6290$; 390 nm, $\varepsilon = 5061$ M^{-1} cm^{-1}), which reflects the interaction of the lone pair electrons with the conjugated π system.[27] The IR spectrum of **1a** has a carbonyl stretch at 1673 cm^{-1} which, upon deprotonation, shifts to 1637 cm^{-1}, indicative of a delocalization of the negative charge about the carbonyl and the naphthalanoid ring system. This observation is consistent with the bathochromatic shift in the electronic absorption spectrum upon deprotonation of **1a**, as delocalization of the charge about the ring generates quinoid resonance forms that have absorption bands in the near UV and visible spectral regions.

Coordination of deprotonated **1a** to a ferric center results in a shift of the carbonyl stretch to 1580 cm^{-1}, indicative of a metal–oxygen bonding interaction with the hydroximate functionality.[28,29] Chelation of the hydroxamate linkage to Fe(III) suggests an electronic structure that is most closely related to that of Fe(III) hydroxamates and catecholates, where two sets of ligand-to-metal charge transfer transitions are observed, ($\lambda_{max} = 330$ and $\lambda_{max} = 550$–430 nm) deriving from metal–oxygen out-of-plane π-bonding interactions.[28,30–32] Indeed, the electronic absorption spectrum of **1b** possesses a broad absorption feature centered at 430 nm ($\varepsilon = 6290$ M^{-1} cm^{-1}) and a higher energy transition at 345 nm ($\varepsilon = 11\,573$ M^{-1} cm^{-1}) which derive from oxygen-to-iron ligand-to-metal charge transfer (LMCT) transitions (Fig. 1). As a result, the photoreactivity of **1b** upon photolysis at $\lambda \geqslant 345$ and $\lambda \geqslant 455$ nm is similar, however, the higher energy transition possesses a considerably larger extinction and quantum yield for reactivity ($\phi_{365} = 2.1 \times 10^{-4}$, $\phi_{436} = 3.6 \times 10^{-5}$).[17]

Photolysis of 1a

Low temperature photoreactivity. Photolysis of **1a** in an ethanol matrix with $\lambda \geqslant 345$ nm at 4 K yields the EPR spectrum shown in Fig. 2(a). The clear 6-line pattern and half-field transition indicate that an $S = 1$ diradical intermediate is generated upon photolysis.[23,33,34] The irreversible changes associated with warming the sample to temperatures above 30 K indicate a chemical reaction has occurred. Both the asymmetric splitting pattern and hyperfine coupling constant (a_N)[24] of the new signal measured at 77 K ($a_N = 23$ G) are solvent independent[25] and are very similar to those observed for simple nitroxyl radicals in both the presence[25,35–38] and absence[33,39–43] of paramagnetic metal ions. However, the observed intensity relationship within the 3-line pattern (2 : 4.5 : 1) does vary somewhat from that reported for nitroxyl radicals at 77 K.[33,39–43] Cooling the sample from 77 to 4 K yields a spectrum that is devoid of a half-field transition but exhibits a sharp signal centered at $g = 2.0035$ that is superimposed upon a very broad and ill-defined feature [Fig. 2(c)]. The broad component may also be attributed to absorption from a nitroxyl radical exhibiting a slow spin relaxation time at 4 K.[37,44,45] Based on the temperature dependence of the EPR signal, a diradical intermediate is formed upon photolysis of **1a** at 4 K [Fig. 2(a)] and subsequently reacts with the matrix at temperatures above *ca.* 30 K to yield the spectrum observed at 77 K [Fig. 2(b)]. This spectral profile can be fit as a nitroxyl radical superimposed upon an isolated matrix radical. In accordance with the mechanistic work on the

photochemical degradation of 1,2,3-benzotriazine systems,[46,47] and the previously observed stepwise photochemical release of N_2 from similar ring systems,[48,49] the observed spectrum at 4 K [Fig. 2(a)] can be assigned to the ring-opened diradical structure **2a** (Scheme 1). This structure is also consistent with the zero field splitting parameters calculated from the spectrum using the point dipole approximation. Upon warming, **2a** reacts to yield the highly unstable diradical **3a**[50] that then rapidly abstracts an H-atom from the matrix to yield the nitroxyl radical **4a** which is observed at 77 K (Scheme 1).

Photoreactivity in solution. Excitation of **1a** ($\lambda = 355$ nm) in 2-propanol yields two transients, the first of which has a similar wavelength profile to that observed for photolysis of **1a** in acetonitrile. In 2-propanol, this transient is rapidly quenched to generate a second intermediate with a single absorption maximum at 380 nm that decays biexponentially. The rapid quenching of the transient species that is observed in 2-propanol (Fig. 4, inset) has two potential origins: either an H-atom abstraction pathway *via* a diradical intermediate (*cf.* Fig. 2), or a proton transfer mechanism that is reflective of the acid/base chemistry of the intermediate. The absence of quenching in dry acetonitrile is key to the elucidation of the photochemistry observed in 2-propanol. When 10 molar equivalents of water are added as a proton source to dry acetonitrile, the same rapid quenching of the transient is indeed observed (Fig. 5), indicating that the intermediate is basic under these conditions. A Stern–Volmer treatment of the quenching process yields a rate constant $k_q = 2.20 \times 10^7$ M^{-1} s^{-1} ($R^2 = 0.95$),[51] indicating the observed quenching is a diffusional process. Since the spectral profile suggests that the first species observed upon photolysis of **1a** is a chromophore with both ketene ($\lambda_{max} \approx 380$ nm)[52] and oxime functionalities within an *o*-quinoid skeleton ($\lambda_{max} \approx 440$ nm),[49,53–60] the transient species is assigned as the oxime ketene (**5**), where protonation at the imine nitrogen is responsible for the quenching observed in 2-propanol (Scheme 1). This is consistent with previous reports on the thermal and photochemical decomposition mechanisms of 1,2,3-benzotriazine systems.[61] Since the pKa of a terminal imine nitrogen is *ca.* 12–14,[49,62] and 2-propanol has a pKa of 16.5,[63] the protonation step that is responsible for the observed quenching must derive from residual water in the 2-propanol solvent.

Once protonated, **5** rearranges to yield a highly unstable species that forms and decomposes within 100 ns to produce the ketene **6** (Scheme 1). The ketene **6** has an absorption profile with a maximum at 380 nm that decays biexponentially.[52,56] The observed biexponential kinetics require a mechanism that involves multiple decomposition pathways,[64] employing both an equilibrium process with the valence tautomeric ring closed form[61,65] and a quenching reaction with 2-propanol to form isopropyl *o*-hydroxyaminobenzoate (**7**) (Scheme 1). The temporal profile can be satisfactorily fit using a parallel reaction mechanism that contains an element of reversibility[66–70] of the general form:

$$A \underset{k_{-1}}{\overset{k_1}{\rightleftharpoons}} B \quad (1)$$

$$A \xrightarrow{k_2} C \quad (2)$$

$$A(t) = C_1 e^{-\lambda_1 t} + C_2 e^{-\lambda_2 t} \quad (3)$$

where λ_1 and λ_2 are composite quantities that represent the three competing rates.[71] Although a unique solution for the fit of the data exists for the parameters $\lambda_1 = 1.7 \times 10^6$ s^{-1} and $\lambda_2 = 1.5 \times 10^5$ s^{-1}, the fact that these parameters are a convoluted function of k_1, k_{-1} and k_2 does not allow the extraction of a unique solution for the individual rate constants.[66,67,70] Empirically, however, the individual rate constants (10^5–10^6 s^{-1}) can only vary by less than an order of

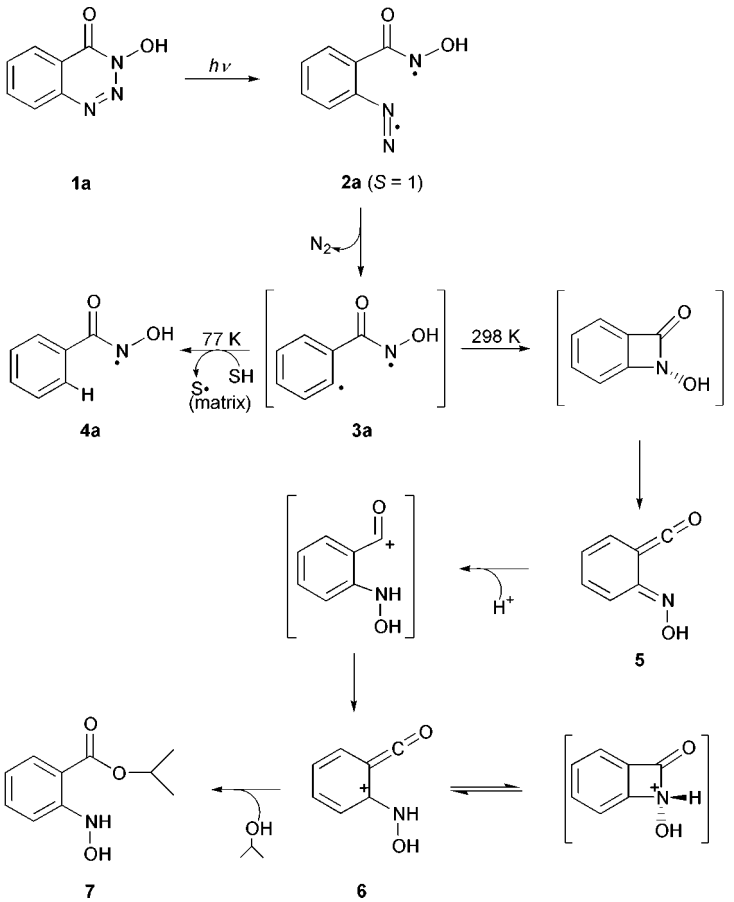

Scheme 1 Proposed photoreactivity of **1a** after excitation ($\lambda \geqslant 345$ or $\lambda = 355$ nm) in both a matrix environment (77 K), and solution (298 K).

magnitude in order to maintain the quality of the fit. The descriptions of the kinetics and spectral data are consistent with the both isolation of the nucleophilic adduct **7** in a 65% yield from the bulk photolysis of **1a** in 2-propanol and the previously reported reactivity of 1,2,3-triazine systems.[61]

Photolysis of 1b

Low temperature photoreactivity. In contrast to the photolysis of **1a**, excitation of **1b** ($\lambda \geqslant 345$ nm) at 4 K in a benzonitrile–2-MeTHF matrix results in the formation of an EPR silent species in the $g \approx 2$ region [Fig. 6(a)].[25] Warming the sample to 77 K with no additional photolysis results in a spectrum that is nearly identical to that observed for the photolysis of **1b** at 77 K [Fig. 2(b) and 6(b)]. Since warming to 77 K with no additional photolysis yields a new monoradical EPR signal at $g = 2.0035$, the EPR silent species at 4 K may be either a zwitterion or an $S = 0$ ligand diradical. Since the reactivity of a zwitterion cannot produce a monoradical upon warming, this species can be eliminated as the initial intermediate produced by the photolysis of **1b** at 4 K. Although no structural information can be obtained regarding the EPR silent species, the formation of a spectral signature similar to that of a nitroxyl monoradical at 77 K suggests that the EPR silent species at 4 K is indeed an $S = 0$ ligand diradical intermediate. The well-documented instability of phenyl radicals in hydrocarbon matrices[50] necessitates the assignment of the 4 K species to that of **2b**, which, upon warming, reacts with the matrix to yield the monoradical **4b** observed at 77 K (Scheme 2). Although the formation of Fe(II) is detected upon photolysis of **1b** in solution, photolysis of **1b** in the matrix at 77 K reveals no bleaching of the optical spectrum, indicating that Fe(II) is not initially formed upon photolysis and is produced by the subsequent reactivity of the intermediates.

Photoreactivity in solution. Excitation of **1b** in benzonitrile ($\lambda = 355$ nm) yields a single transient that begins to form 240 ns after the pulse and has three absorption features at 390, 430 and 740 nm that decay monoexponentially (Fig. 7). The temporal profile of the intermediate (Fig. 7, inset) has several interesting features. First, growth of the transient signal does not begin until 240 ns after the excitation pulse, indicating the presence of intermediates with electronic spectra similar to that of the ground state compound. To account for the delayed rise, the temporal profile was fitted as the third species in a reaction sequence of the general form:[70]

$$A \xrightarrow{k_1} B \xrightarrow{k_f} C \xrightarrow{k_d} D \tag{4}$$

$$C_{(t)} = A_0 k_1 k_f \left[\frac{e^{-k_1 t}}{(k_f - k_1)(k_d - k_1)} + \frac{e^{-k_f t}}{(k_f - k_1)(k_d - k_f)} - \frac{e^{-k_d t}}{(k_d - k_1)(k_d - k_f)} \right] \tag{5}$$

where $k_1 \geqslant 10^6$ s^{-1},[72] $k_f = 1.6 \times 10^6$ s^{-1}, $k_d = 5.2 \times 10^5$ s^{-1} and the first two intermediates (A = **3b** , B = **8**) do not con-

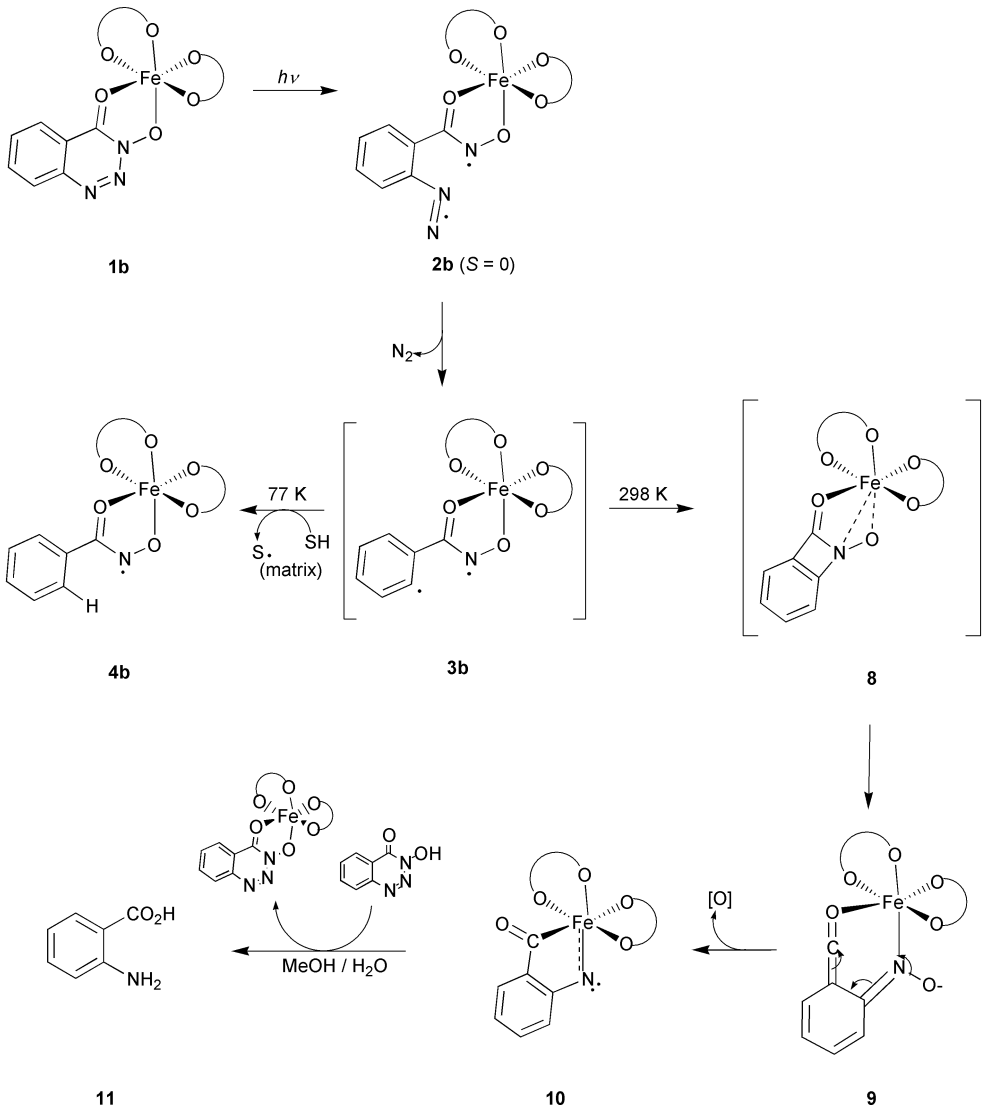

Scheme 2 Proposed mechanism for the reactivity of **1b** after excitation ($\lambda \geqslant 345$ or $\lambda = 355$ nm) in either a benzonitrile–2-MeTHF matrix (77 K) or benzonitrile solution (298 K) including subsequent product isolation steps.

tribute significantly to a change in the optical density at the experimental wavelength (Scheme 2). Secondly, the temporal profile is unaffected by the addition of a variety of quenchers such as O_2, 20 molar equivalents (20–40 mM) of 2-propanol, phenylisocyanate, methanol, $Fe(SO_4)\cdot 7H_2O$, or 3-propene-2-one-4-ol (Hacac). The absence of quenching upon addition of O_2 eliminates the possibility of a triplet excited state or radical species as the observed transient, while the lack of reactivity with Fe^{2+} excludes a bimolecular redox reaction and the addition of Hacac eliminates a ligand exchange reaction.

The transient absorption results and the product analyses (*vide infra*) lead to the following description of the photochemical decomposition of **1b** in benzonitrile. Upon photolysis of **1b**, a diradical intermediate is produced that is structurally similar to that observed for the photodecomposition of **1a**. The diradical **2b** (Scheme 2) loses N_2 and collapses to form a four membered lactam ring **8**, which has been widely cited in reference to decomposition of 1,2,3-benzotriazine systems.[61] Once formed, **8** will not exhibit a ligand centered absorption within the experimental window since the lowest energy π–π* transition of this ring system is at *ca.* 270 nm.[55] The lactam ring can subsequently open to the coordinated oxime ketene **9** [species C in eqn. (4)],[73] which is detected *via* the rise ($k_f = 1.6 \times 10^6$ s^{-1}) and decay ($k_d = 5.2 \times 10^5$ s^{-1}) of the absorbance at 390 and 440 nm. The lack of a quenching product upon photolysis of **1b** indicates that the evolving transient must be coordinated to the metal center and thus would be sterically protected from bimolecular attack by isocyanates and alcohols. Additionally, the peak at 740 nm may be attributed to an oxygen-to-iron LMCT transition within the transient intermediate, **9**, that has been red-shifted by imine nitrogen coordination to the metal.[30,74] Considering the literature precedent for oxygen atom loss in the thermolysis of **1a**[75,76] and coordinated oximes,[77–79] we propose that the decay of **9** involves loss of an oxygen atom and a concerted rearrangement to metallocycle **10**.[80–84] Importantly, no new organic species are detected by conventional chromatography, indicating that the photolysis products are indeed bound to the iron center. As a result, 2-aminobenzoic acid (**11**) could be isolated (73%) only after removal of the metal by the addition of three equivalents of **1a** to a suspension of crude photoproduct. The structure of the product, **11**, confirms that the excitation of **1b** ultimately leads to a ligand-centered photoreaction that is similar to that observed upon photolysis of free ligand **1a**.

Our results document that photolysis of either **1a** or the Fe(III) compound **1b** leads to the formation of $S = 1$ or $S = 0$ diradical intermediates, respectively, that persist only at temperatures below 30 K and react in solution at room temperature within *ca.* 200 ns of initiation. Detection of the diradical intermediates suggests that photolysis of both ligand and metal complex generate an excited state that promotes homolysis of the N–N bond adjacent to the –N=N– unit. For **1**, this state is likely n–π* in nature.[85] However, formation of the diradical intermediate upon photolysis of **1b** reveals that the initially prepared LMCT excited state contains either considerable ligand character, or decays rapidly to a ligand localized excited state that releases N_2. The results presented herein do not allow distinction between these possibilities. These pathways are in contrast to the traditional mechanism that is usually invoked to explain the photochemistry of complexes such as $[Fe(ox)_3]^{3-}$ ($ox = [C_2O_4]^{2-}$) where direct excitation into a LMCT transition leads to homolysis of the Fe–O bond and reduction of the metal center to yield Fe^{2+}.[86]

In consideration of the photoreactivities of **1a** and **1b** toward solution substrates, the first species produced upon photolysis of **1a** is the oxime ketene **5** formed from the diradical **3a** which has undergone unimolecular recombination *via* formation of the 4-membered β-lactam ring within 10 ns. The short lifetime of the diradical intermediate **3a** mandates that, unless the molecule is bound to a DNA substrate, the diradical intermediate cannot be the species responsible for degradation of DNA, since insufficient time exists for a diffusion-controlled bimolecular reaction to occur in solution. In contrast, the ketene intermediate, though unstable and susceptible to nucleophilic attack, possesses considerably retarded decay kinetics relative to the diradical intermediate and could therefore, as illustrated by 2-propanol quenching, participate in bimolecular reactions to yield alkylated or modified DNA products.

The kinetics for formation and decay of the metal-coordinated ketene intermediate **9** do not innocently parallel those for the same intermediate formed upon photolysis of the free ligand. Rather, the formation rate is somewhat slower due to the steric strain involved in forming the 4-membered lactam ring with the metal bound at the adjacent hydroxymate functionality. This effectively increases the diradical (**3b**) lifetime and increases the potential for H-atom abstraction or addition reactions that involve the $S = 0$ ligand diradical and DNA substrates. Moreover, the metal-bound ketene intermediate is more stable than its uncoordinated counterpart, as it is resistant to quenching by nucleophiles and only decays by oxygen atom loss. These results suggest that DNA modification by **1b** likely proceeds *via* the diradical intermediate, but a bimolecular oxidation step, as observed in the photolytic deoxygenation of heterocyclic *N*-oxides,[87] cannot be ruled out.

Conclusions

We show that the photochemical decomposition of 3-hydroxy-1,2,3-benzotriazine-4(3*H*)-one and tris[3-hydroxy-1,2,3-benzotriazine-4(3*H*)-one]iron(III) initially occurs *via* N_2 loss to yield a diradical intermediate that decays rapidly to a ketene in room temperature solution. The excited state that gives rise to the homolytic cleavage of the N–N bond in the Fe(III) complex is ligand-to-metal charge transfer in nature, but the reactivity is not derived from typical homolytic Fe–O bond cleavage. Rather, a ligand localized excited state is produced by either an excited state decay pathway or through direct excitation where the initial LMCT state is more delocalized and has considerable ligand character. The kinetics for the decay of the ketene *via* a 4-membered β-lactam intermediate are influenced by steric contributions associated with the metal complex. The retardation in the rate of formation of this species translates into an extended solution lifetime for the diradical intermediate. Overall, the results have broad implications for the fundamental mechanistic aspects of inorganic and organic photochemistry, as well as applications to the burgeoning fields of photomedicine and environmentally relevant photochemical transformations.

Acknowledgements

We thank Professors Joseph Gajewski and Josef Zwanziger for helpful discussions. The generous support of the American Cancer Society (RPG-99-156-01-C), the Donors of the Petroleum Research Fund (PRF #33340-G4), administered by the American Chemical Society and Research Corporation (Research Innovation Award #RI0102 for J. M. Z.) are gratefully acknowledged.

References and notes

1 U. Duerr and H. Kisch, *Synlett*., 1997, 1335.
2 M. P. Doyle, M. A. McKervey and T. Ye, *Modern Catalytic Methods for Organic Synthesis with Diazo Compounds: From Cyclopropanes to Ylides*, Wiley, New York, 1998.

3 L. E. Kaim and C. Meyer, *J. Org. Chem.*, 1996, **61**, 1556.
4 A. Reiser, *Photoreactive Polymers: The Science and Technology of Resists*, Wiley, New York, 1989.
5 G. Pohlers, J. C. Scaiano, E. Step and R. Sinta, *J. Am. Chem. Soc.*, 1999, **121**, 6167.
6 S. J. Gould, N. Tamayo, C. R. Melville and M. C. Cone, *J. Am. Chem. Soc.*, 1994, **116**, 2207.
7 S. Mithani, G. Weeratunga, N. J. Taylor and G. I. Dmitrienko, *J. Am. Chem. Soc.*, 1994, **116**, 2209.
8 B. G. Maiya, C. V. Ramana, S. Arounaguiri and M. Nagarajan, *Bioorg. Med. Chem. Lett.*, 1997, **7**, 2141.
9 P. A. Wender, S. M. Touami, C. Alayrac and U. C. Philipp, *J. Am. Chem. Soc.*, 1996, **118**, 6522.
10 S. M. Touami, C. C. Poon and P. A. Wender, *J. Am. Chem. Soc.*, 1997, **119**, 7611.
11 K. Nakatani, S. Maekawa, K. Tanabe and I. Saito, *J. Am. Chem. Soc.*, 1995, **117**, 10635.
12 M. J. Cohn, C. L. Xie, J. P. M. Tuchagues, C. G. Pierpont and D. N. Hendrickson, *Inorg. Chem.*, 1992, **31**, 5028.
13 A. Sokolowski, J. Mueller, T. Weyhermueller, R. Schnepf, P. Hildebrandt, K. Hildenbrand, E. Bothe and K. Wieghardt, *J. Am. Chem. Soc.*, 1997, **119**, 8889.
14 A. Sokolowski, H. Leutbecher, T. Weyhermuller, R. Schnepf, E. Bothe, E. Bill, P. Hildebrandt and K. Wieghardt, *J. Biol. Inorg. Chem.*, 1997, **2**, 444.
15 V. Balzani, A. Credi and M. Venturi, *Coord. Chem. Rev.*, 1998, **171**, 3.
16 K. E. Erkkila, D. T. Odom and J. K. Barton, *Chem. Rev.*, 1999, **99**, 2777.
17 T. D. Maurer, B. J. Kraft, S. M. Lato, A. D. Ellington and J. M. Zaleski, *Chem. Commun.*, 2000, 69.
18 D. P. Arya and D. J. Jebaratnam, *J. Org. Chem.*, 1995, **60**, 3268.
19 H. J. Eppley, S. A. Lato, A. D. Ellington and J. M. Zaleski, *Chem. Commun.*, 1999, 2405.
20 K. Kuma, J. Tanaka, K. Mastunaga and K. Mastunaga, *Limnol. Oceanogr.*, 2000, **45**, 1235.
21 F. Neese, *QCPE Bull.*, 1995, **5**, 15.
22 B. J. Gaffney and H. J. Silverstone, in *Biological Magnetic Resonance*, ed. J. Reuben and J. Berliner, Plenum Press, New York, 1993, vol. 13, p. 1.
23 D. A. Dougherty, in *Matrix Isolation EPR Spectroscopy of Biradicals*, ed. M. S. Platz, Plenum, New York, 1990, pp. 117–142.
24 Assignment of $a_{\|}$ in axially symmetric nitroxyl radicals at 77 K is defined as twice the separation of the two outermost transitions (see ref. 33). We report this value as a_N. This coupling and asymmetric pattern is observed in multiple solvent systems including, ethanol, 2-methyltetrahydrofuran and toluene.
25 S. S. Eaton and G. R. Eaton, *Coord. Chem. Rev.*, 1978, **26**, 207.
26 As a result of the large amount of unreacted iron(III), a large $S = 5/2$, $g = 4.3$ EPR signal is persistent after photolysis, but no additional EPR signals are observed.
27 R. M. Silverstein, G. C. Bassler and T. C. Morrill, *Spectrometric Identification of Organic Compounds*, 4th edn., John Wiley & Sons, New York, 1981.
28 M. K. Das and N. Roy, *Indian J. Chem., Sect. A*, 1986, **25**, 246.
29 R. M. Silverstein, G. C. Bassler and T. C. Morril, *Spectrometric Identification of Organic Compounds*, 5th edn., Wiley, New York, 1991.
30 T. B. Karpishin, M. S. Gebhard, E. I. Solomon and K. N. Raymond, *J. Am. Chem. Soc.*, 1991, **113**, 2977.
31 D. D. Cox, S. J. Benkovic, L. M. Bloom, F. C. Bradley, M. J. Nelson, L. Que, Jr. and D. E. Wallick, *J. Am. Chem. Soc.*, 1988, **110**, 2026.
32 K. Abu-Dari and K. N. Raymond, *J. Am. Chem. Soc.*, 1977, **99**, 2003.
33 J. E. Wertz and J. R. Bolton, *Electron Spin Resonance Elementary Theory and Practical Applications*, 2nd edn., Chapman and Hall, New York, 1986.
34 W. Gordey, *Theory and Applications of ESR*, Wiley & Sons, New York, 1985, vol. 15.
35 S. S. Eaton and G. R. Eaton, *Coord Chem. Rev.*, 1988, **83**, 29.
36 M. H. Rakowsky, A. Zecevic, G. R. Eaton and S. S. Eaton, *J. Magn. Reson.*, 1998, **131**, 97.
37 M. Seiter, V. Budker, J. L. Du, G. R. Eaton and S. S. Eaton, *Inorg. Chim. Acta*, 1998, **273**, 354.
38 M. C. R. Symons, D. X. West and J. G. Wilkinson, *J. Organomet. Chem.*, 1975, **102**, 213.
39 S. Bhattacharjee, M. N. Khan, H. Chandra and M. C. R. Symons, *J. Chem. Soc., Perkin Trans. 2*, 1996, 2631.
40 O. Brede and V. Zubarev, *J. Chem. Soc., Perkin Trans. 2*, 1994, 1821.
41 H. D. L. Shields, Terence, Chiu, FonJen and J. Phillip Hamrick, Jr., *J. Chem. Phys.*, 1982, **77**, 4333.
42 H. A. Gottinger, V. E. Zubarev and O. Brede, *J. Chem. Soc., Perkin Trans. 2*, 1997, 2167.
43 A. A. McConnell, S. Mitchell, A. L. Porte, J. S. Roberts and C. Thomson, *J. Chem. Soc. B*, 1970, 833.
44 C. P. Poole, Jr., *Electron Spin Resonance: A Comprehensive Treatise on Experimental Techniques*, 2nd edn., Wiley, New York, 1966.
45 M. Jinguji, T. Imamura, H. Murai and K. Obi, *Chem. Phys. Lett.*, 1981, **84**, 335.
46 G. Ege, *Chem. Ber.*, 1968, **101**, 3079.
47 G. Ege and F. Pasedach, *Chem. Ber.*, 1968, **101**, 3089.
48 L. C. Bush, L. Maksimovic, X. W. Feng, H. S. M. Lu and J. A. Berson, *J. Am. Chem. Soc.*, 1997, **119**, 1416.
49 H. Wang, C. Bruda, G. Persy and J. Wirz, *J. Am. Chem. Soc.*, 2000, **122**, 5849.
50 The instability of phenyl radicals in hydrocarbon matrices is well documented and their direct observation at low temperatures typically requires inert matrices. For examples, see: A. V. Friderichsen, J. G. Radziszewski, M. R. Nimlos, P. R. Winter, D. C. Dayton, D. E. David and G. B. Ellison, *J. Am. Chem. Soc.*, 2001, **123**, 1977; M. Vala, J. Szczepanski, F. Pauzat, O. Parisel, D. Talbi and Y. Ellinger, *J. Phys. Chem.*, 1994, **98**, 9187.
51 In light of the convoluted kinetics scheme [eqn. (1)–(3)], the absolute value of k_q needs to be considered as an approximation.
52 N. S. Isaacs and E. Rannala, *J. Chem. Soc., Perkin Trans. 2*, 1975, 1555.
53 J. C. Scaiano, V. Wintgens and J. C. Netto-Ferreira, *Pure Appl. Chem.*, 1990, **62**, 1557.
54 S. Nagakura and A. Kubyama, *J. Am. Chem. Soc.*, 1953, **76**, 1003.
55 J. Morawietz, W. Sander and M. Traubel, *J. Org. Chem.*, 1995, **60**, 6368.
56 A. Krantz, *J. Am. Chem. Soc.*, 1974, **96**, 4992.
57 S. V. Kessar, A. K. S. Mankotia, J. C. Scaiano, M. Barra, J. Gebicki and K. Huben, *J. Am. Chem. Soc.*, 1996, **118**, 4361.
58 T. Nogami, T. Hishida, M. Yamada, H. Mikawa and Y. Shirota, *Bull. Chem. Soc. Jpn.*, 1975, **48**, 3709.
59 V. Wintgens, C. Netto-Ferreira, Casal and J. C. Scaiano, *J. Am. Chem. Soc.*, 1990, **112**, 2363.
60 K. L. Tseng and J. Michl, *J. Am. Chem. Soc.*, 1977, **99**, 4840.
61 H. Neunhoeffer and P. F. Wiley, in *Chemistry of 1,2,3-Traizines and 1,2,4-Triazines, Tetrazines and Pentazines*, ed. A. Weissberger and E. C. Taylor, Wiley & Sons, New York, 1978, vol. 33, pp. 50–60.
62 D. C. Harris, *Quantitative Chemical Analysis*, 4th edn., Freeman & Co., New York, 1995.
63 J. March, *Advanced Organic Chemistry*, 4th edn., Wiley & Sons, New York, 1996.
64 Since there is no evidence for a dimerization of **5** or a reaction with **1a** in the ground state, and the major product **7** was generated through a bimolecular reaction with the solvent (excess), a 2nd order dependence on **5**, or **5** and **1a** was eliminated from the mechanism.
65 J. L. Segura and N. Martin, *Chem. Rev.*, 1999, **99**, 3199.
66 C. Capellos and B. H. J. Bielski, *Kinetic Systems*, Huntington, New York, 1980.
67 J. H. Espenson, *Chemical Kinetics and Reaction Mechanisms*, McGraw-Hill, New York, 1981.
68 J. J. Russell, J. A. Seetula, D. Gutman, F. Danis, F. Caralp, P. D. Lightfoot, R. Lesclaux, C. F. Melius and S. M. Senkan, *J. Phys. Chem.*, 1990, **94**, 3277.
69 I. R. Slagle, E. Ratajczak, M. C. Heaven, D. Gutman and A. F. Wagner, *J. Am. Chem. Soc.*, 1985, **107**, 1838.
70 K. A. Connors, *Chemical Kinetics*, VCH, New York, 1990.
71 $\lambda_1 = 0.5 \times [(k_1 + k_{-1} + k_2) + \{(k_1 + k_{-1} + k_2)^2 - 4k_1k_2\}]$,
$\lambda_2 = 0.5 \times [(k_1 + k_{-1} + k_2) - \{(k_1 + k_{-1} + k_2)^2 - 4k_1k_2\}]$
72 Due to the inability to observe **8**, an exact measure of the decay constant for this species is unattainable, however the induction period for the formation of **9** necessitates an appreciable solution lifetime (see ref. 70, p. 75).
73 Opening of the lactam ring could result in either a *syn* or *anti* configuration about the nitrogen–carbon π-bond. If the *syn* isomer were the dominant form in solution, 1,2-benzisoxazol-3(1*H*)-one would be formed in high yield by the nucleophilic attack of the oxime oxygen on the ketene carbon. Since photolysis of **1a** and **1b** does not produce this species in high yield, the *anti* isomer bound through the imine nitrogen, is proposed to be the dominant form of **9** in solution (see H. Tomioka, N. Ichikawa and K. Komatsu, *J. Am. Chem. Soc.*, 1992, **114**, 8045).
74 K. Ramesh and R. Mukherjee, *J. Chem. Soc., Dalton Trans.*, 1992, 83.

75 P. Ahern, T. Navratil and K. Vaughn, *Tetrahedron Lett*., 1973, **46**, 4547.
76 P. Ahern, T. Navratil and K. Vaughn, *Can. J. Chem*., 1977, **55**, 630.
77 V. Y. Kukushkin, D. Tudela and A. J. L. Pombeiro, *Coord. Chem. Rev*., 1996, **156**, 333.
78 H. Alper and J. T. Edward, *Can. J. Chem*., 1970, **48**, 1543.
79 J. Charalambous, L. I. B. Haines, J. S. Morgan, D. S. Peat, M. J. M. Campbell and J. Bailey, *Polyhedron*, 1987, **6**, 1027.
80 K. Badyal, W. R. McWhinnie, T. A. Hamor and H. Chen, *Organometallics*, 1997, **16**, 3194.
81 S. R. Berryhill and M. Rosenblum, *J. Org. Chem*., 1984, **45**, 1984.
82 S. R. Berryhill, T. Price and M. Rosenblum, *J. Org. Chem*., 1983, **48**, 158.
83 S. Javaheri and W. P. Glering, *Organometallics*, 1984, **3**, 1927.
84 J. P. Collman, L. S. Hegehus, J. R. Norton and R. G. Finke, *Principles and Applications of Organotransition Metal Chemistry*, University Science Books, Mill Valley, CA, 1987.
85 N. J. Turro, *Modern Molecular Photochemistry*, Benjamin/Cummings, London, 1978.
86 J. Sima and J. Makanova, *Coord. Chem. Rev*., 1997, **160**, 161.
87 J. S. Daniels, T. Chatterji, L. R. MacGillivray and K. S. Gates, *J. Org. Chem*., 1998, **63**, 10027.